ILLUMINATING BLACK HOLE BINARY FORMATION CHANNELS WITH SPINS IN ADVANCED LIGO

The Astrophysical Journal Letters, 832:L2 (7pp), 2016 November 20 doi:10.3847/2041-8205/832/1/L2

ILLUMINATING BLACK HOLE BINARY FORMATION CHANNELS WITH SPINS IN ADVANCED LIGO

Carl L. Rodriguez[1,2], Michael Zevin[2], Chris Pankow[2], Vasilliki Kalogera[2], and Frederic A. Rasio[2]
[1] MIT-Kavli Institute for Astrophysics and Space Research, 77 Massachusetts Avenue, 37-664H, Cambridge, MA 02139, USA
[2] Center for Interdisciplinary Exploration and Research in Astrophysics (CIERA) and Department of Physics and Astronomy, Northwestern University, 2145 Sheridan Road, Evanston, IL 60208, USA
Received 2016 September 18; accepted 2016 October 17; published 2016 November 11

ABSTRACT

The recent detections of the binary black hole mergers GW150914 and GW151226 have inaugurated the field of gravitational-wave astronomy. For the two main formation channels that have been proposed for these sources, isolated binary evolution in galactic fields and dynamical formation in dense star clusters, the predicted masses and merger rates overlap significantly, complicating any astrophysical claims that rely on measured masses alone. Here, we examine the distribution of spin–orbit misalignments expected for binaries from the field and from dense star clusters. Under standard assumptions for black hole natal kicks, we find that black hole binaries similar to GW150914 could be formed with significant spin–orbit misalignment only through dynamical processes. In particular, these heavy-black hole binaries can only form with a significant spin–orbit *anti*-alignment in the dynamical channel. Our results suggest that future detections of merging black hole binaries with measurable spins will allow us to identify the main formation channel for these systems.

Key words: binaries: general – gravitational waves – stars: black holes – supernovae: general

1. INTRODUCTION

The gravitational-wave detections GW150914 and GW151226 are the first direct evidence of the formation and merger of stellar-mass binary black holes (BBHs) in the local universe (Abbott et al. 2016a, 2016b). Although many channels have been explored for the formation of such systems, most proposals fall into two categories: the "field" channel, in which BBHs are formed from isolated stellar binaries, usually involving either a common-envelope phase (e.g., Voss & Tauris 2003; Dominik et al. 2012, 2013; Belczynski et al. 2016) or chemically homogeneous evolution due to rapid stellar rotation (e.g., De Mink & Mandel 2016; Mandel & De Mink 2016; Marchant et al. 2016), or the "dynamical" channel, in which BBHs are created though three-body encounters in dense star clusters (e.g., Sigurdsson & Hernquist 1993; Portegies Zwart & Mcmillan 2000; Downing et al. 2010, 2011; Ziosi et al. 2014; Rodriguez et al. 2015, 2016a). Unfortunately, the masses and merger rates predicted by these models often significantly overlap, making it difficult to discriminate between different formation channels for BBHs even with multiple detections.

However, masses and merger rates are not the only observable predictions from BBH formation models. In particular, the distribution of BH spin orientations are expected to depend heavily on the binary formation mechanism. For BBHs from the field, it is expected that the individual BH spins should be mostly aligned with the orbital angular momentum (Kalogera 2000), with any misalignment arising from the momentum "kick" imparted to the orbit during core collapse. For dynamically formed BBHs, both the spin and orbital angular momenta should be randomly distributed on the sphere. These spin–tilt misalignments produce relativistic precession of the orbit, which can be detected through the amplitude modulations in the gravitational waveform as the binary changes its orientation with respect to the detector (Apostolatos et al. 1994; Vitale et al. 2014).

In this Letter, we compare the expected distributions of spin–tilt misalignments for binaries formed from isolated binary stellar evolution to those formed from dynamical encounters in dense star clusters. We find that, for sufficiently massive systems (such as GW150914), measurements of the BBH spin–tilt will allow LIGO to discriminate between dynamically and field-formed binaries. In addition, we find that dynamics provides the best route to forming binaries with a significant component of the spins anti-aligned with the orbital angular momentum. Since Advanced LIGO can best constrain the component of the spin angular momentum that is aligned with the orbital angular momentum (Abbott et al. 2016c and references therein), we suggest that this may represent the best way to differentiate these BBH populations.

2. SPIN–ORBIT MISALIGNMENT

In Figure 1, we show the vectors and angles that describe the spin orientations of a BBH system. For any binary in which the total spin vector, $\boldsymbol{S}$, is misaligned with the orbital angular momentum, $\boldsymbol{L}$, the entire system will precess about the total angular momentum, $\boldsymbol{J}$ (Apostolatos et al. 1994). We refer to the angle between $\hat{L}$ and $\hat{S}$, θ_{LS}, as the spin–orbit misalignment, or the spin–tilt. Although restricting ourselves to only θ_{LS} erases any information about the individual BH spins and their potential resonant configurations (such as those studied in Gerosa et al. 2013a, 2014; Trifirò et al. 2016), it is the component of the mass-weighted spin angular momentum perpendicular to the orbital plane, $\chi_{\rm eff} \equiv \frac{c}{(Gm_1+m_2)}\left[\frac{\boldsymbol{S}_1}{m_1}+\frac{\boldsymbol{S}_2}{m_2}\right]\cdot\hat{L}$, that is best constrained by Advanced LIGO. The components of the spins that lie in the plane of the orbit are responsible for the precession of $\hat{L}$ about $\hat{J}$, which induces modulations in the amplitude of the gravitational waveform; however, the BBHs detected by LIGO have so far not yielded significant constraints on the in-plane spins of merging BHs (Abbott et al. 2016d).

2.1. Misalignments in Isolated Field Binaries

For BBHs formed from stellar binaries in the isolated channel, the primary mechanism for inducing a misalignment between $\boldsymbol{L}$ and $\boldsymbol{S}$ is the change in $\boldsymbol{L}$ imparted by the natal kick

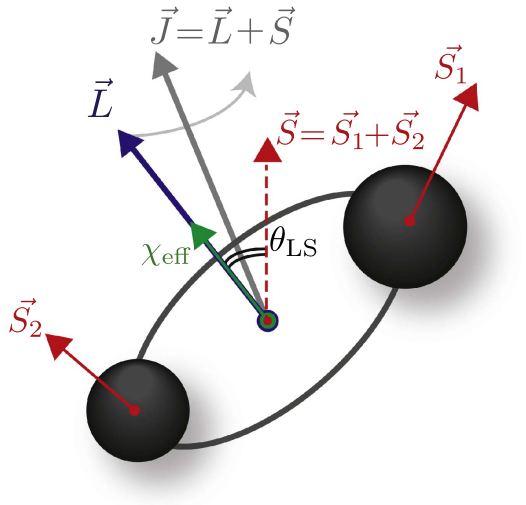

Figure 1. Diagram of the vectors and angles that define the spinning BBH problem. For any system where $\boldsymbol{S}$ and $\boldsymbol{L}$ are misaligned, the orbital plane will precess about the total angular momentum, $\boldsymbol{J}$.

(NK). The change in linear momentum instantaneously imparted to the exploding star, from either emission of neutrinos or an asymmetric explosion mechanism (e.g., Janka 2013), can significantly change the orbit of the binary, resulting in a change to θ_{LS}.

We use the Binary Stellar Evolution (BSE; Hurley et al. 2002) code to create a BBH population representative of the field. BSE uses a series of metallicity-dependent fitted stellar tracks to rapidly model the evolution of stellar populations. For binaries, BSE also models stable and unstable mass transfer, tidal circularization, gravitational-wave emission, and the changes to the orbital angular momentum arising from kicks. In addition, our version of BSE contains several modifications to low-metallicity stellar winds (Vink et al. 2001; Belczynski et al. 2010) and core-collapse supernova (SN; Fryer et al. 2012) required to form "heavy" BBHs such as GW150914 (Abbott et al. 2016b).

Our NK prescription is based on that developed in Fryer et al. (2012). Briefly, we assume that all compact objects receive an NK drawn from a Maxwellian distribution with a dispersion of $\sigma = 265\,{\rm km\,s^{-1}}$ (used to model the observed velocities of pulsars in the galaxy; Hobbs et al. 2005). However, for BHs we also assume that some fraction of the mass ejected during core collapse will "fall back" onto the newly formed proto-compact object. When this happens, conservation of momentum demands that the velocity of the BH be reduced by

$$V_{\rm kick}^{\rm BH} = (1 - f_{\rm fallback})\, V_{\rm kick}^{\rm NS}. \quad (1)$$

The fraction of material that falls back ($f_{\rm fallback}$) is proportional to the core mass of the BH progenitor; for stars with large core masses (those with a carbon–oxygen core mass greater than 11 $M_\odot$), the rapid SN prescription of Fryer et al. (2012) assumes complete fallback of material onto the newly formed BH (i.e., $f_{\rm fallback} = 1$). This approximates the "direct collapse" of BH progenitors with proto-neutron star masses $\gtrsim 3\,M_\odot$ (Fryer & Kalogera 2001). A more massive pre-collapse core will produce a more massive BH, accrete more fallback material, and experience a smaller NK. We can expect that BBHs formed from isolated binaries in the field should show less spin–orbit misalignment, especially as one considers binaries with heavy BH components.

In addition, we consider two additional kick prescriptions for field BBH populations. Our proportional kick prescription assumes a much simpler relationship between the new BH mass and the maximum NS mass, similar to that proposed for neutrino-driven kicks (Janka 2013):

$$V_{\rm kick}^{\rm BH} = \left(\frac{m_{\rm NS}}{m_{\rm BH}}\right) V_{\rm kick}^{\rm NS}, \quad (2)$$

where we assume $m_{\rm NS} = 2.5\,M_\odot$. We also consider the case where BHs receive kicks comparable to those of NSs, i.e.,

$$V_{\rm kick}^{\rm BH} = V_{\rm kick}^{\rm NS}, \quad (3)$$

though as we discuss in Section 4, such kicks represent an extreme assumption not supported by current observations.

In addition to varying the NK magnitudes, we also explore different NK directions. By default, most population synthesis studies have assumed kicks to be evenly distributed in solid angle about the sphere of the exploding star. However, pulsar observations have suggested a correlation between the kick direction and the spin axis of the newly formed proto-compact object (e.g., Wang et al. 2006; Ng & Romani 2007; Kaplan et al. 2008). Therefore, we consider two cases: an isotropic case, where NKs are distributed randomly in solid angle over the sphere of the star, and a polar case, where we assume that all NKs are preferentially launched from a cone with an opening angle of 10° about the spin axis of each star.

For each kick prescription, we consider 11 different stellar metallicities: 1.5 $Z_\odot$, $Z_\odot$, 0.5 $Z_\odot$, 0.375 $Z_\odot$, 0.25 $Z_\odot$, 0.125 $Z_\odot$, 0.05 $Z_\odot$, 0.0375 $Z_\odot$, 0.025 $Z_\odot$, 0.0125 $Z_\odot$, and 0.005 $Z_\odot$. We then evolve 10^5 binaries in each metallicity bin for 50 Myr with BSE. We sample the primary mass from a $p(m)\ dm \propto m^{-2.3}\ dm$ power law from 18 $M_\odot$ to 150 $M_\odot$ (Kroupa 2001), and use a mass ratio distribution flat from 0 to 1. The eccentricities are drawn from a thermal distribution, $p(e)de = 2e\ de$, and the initial semimajor axes from a distribution flat in $\log(a)$ from 10 $R_\odot$ to 10^5 $R_\odot$. We limit our sample to only those BBHs that will merge from emission of gravitational waves in less than 13.8 Gyr.

To assign spin–tilts to each binary, we assume that the only mechanism for misaligning the orbital and spin angular momenta is the NK. Although BSE does not keep track of the three-dimensional spin misalignments during its evolution, we record the angle between the old and new $\hat{L}$ after each NK. The total spin–tilt misalignment is the combination of the two tilts. We emphasize that this is a highly conservative estimate: both mass transfer during the common-envelope phase and tidal forces should realign the spins of the first and second components of the binary between the formation of the first and second BHs. However, this realignment would serve to decrease the large spin–tilts reported here, making the distinction between field and cluster populations even more distinct. See the Appendix for details.

Finally, we evolve each binary from a separation of $r = 1000(m_1 + m_2)G/c^2$ to the separation where the binary enters the LIGO band (10 Hz) using the precession-averaged post-Newtonian evolution in the `Precession` package (Gerosa & Kesden 2016) and assuming maximal spins for the BH components. This was done to report the spin–tilt misalignments

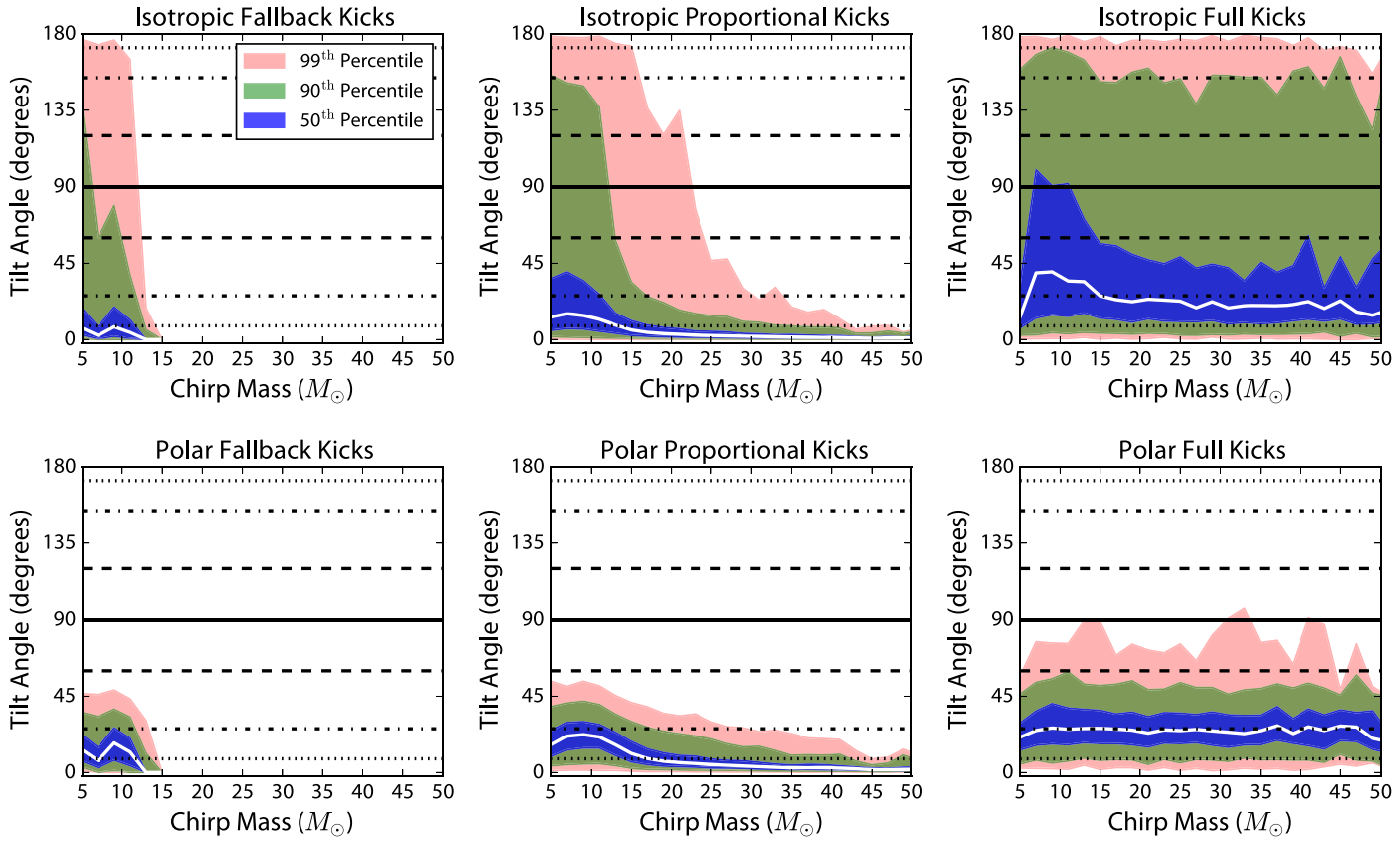

Figure 2. Distributions of spin–tilt misalignments for our field and cluster populations as a function of chirp mass. The colors show the field population, with the solid white line indicating the median value, and the blue, green, and pink regions showing where 50%, 90%, and 99% of sources lie in each 2 $M_\odot$ bin. The distribution of cluster misalignments, evenly distributed in $\sin\theta_{LS}$, is shown in black, with the solid line indicating the median, and the dashed, dotted–dashed, and dotted lines showing the 50%, 90%, and 99% regions, respectively. As we have explicitly assumed no realignment of the spins between NKs, these represent the largest possible spin–tilts from the field (see Figure 5 for less conservative estimates). Note that all binaries above $\sim$15 $M_\odot$ in the fallback prescription have zero spin–tilt misalignment, and are not shown in the plot.

that would be measurable by Advanced LIGO. In practice, the spin–tilt distributions do not change between formation and $r = 1000(m_1 + m_2)G/c^2$, since the couplings between $\hat{S}_1$, $\hat{S}_2$, and $\hat{L}$ are $\mathcal{O}(v^6/c^6)$ corrections to the spin evolution. The differences in θ_{LS} between $r = 1000(m_1 + m_2)G/c^2$ and the separation each binary enters the LIGO band are also minor, but we report the 10 Hz values for comparison with previous results (Gerosa et al. 2013a).

2.2. Cluster Binaries

For BBHs formed in dense stellar environments, we assume the orbital and spin angular momenta are completely random. As more than 99% of all BBHs that merge in the local universe from globular clusters are formed through complicated and chaotic dynamical interactions (Rodriguez et al. 2016a), BBHs from clusters should have $\hat{L}$, $\hat{S}_1$, and $\hat{S}_2$ isotropically distributed across the sphere. We conclude that $p(\theta_{LS})d\theta_{LS} = \sin(\theta_{LS})/2\ d\theta_{LS}$, suggesting that clusters preferentially form binaries with spins lying in the plane of the orbit. Since it has been shown (Bogdanovic et al. 2007; Gerosa et al. 2013b) that an isotropic distribution of BBH spins remains isotropic during inspiral, we assume cluster binaries to have randomly distributed spins when they enter the LIGO band. Note that we are only considering the "classical" channel of dynamical formation; many additional channels have been proposed in which dynamics can induce mergers in BBHs that formed from pre-existing stellar binaries, such as those driven to merger via Kozai–Lidov oscillations from either stellar-mass triples (e.g., Silsbee & Tremaine 2016) or binaries orbiting a supermassive BH (e.g., Antonini & Perets 2012; VanLandingham et al. 2016), or from binaries that form and potentially accrete gas in AGN disks (e.g., Bartos et al. 2016; Stone et al. 2016). Although the spin distributions of such scenarios are worthy of future study, for simplicity we do not consider them here.

3. RESULTS

Because the magnitude of the BH NK decreases with increasing BH mass, we are most interested in the correlation between the spin–tilts and the binary masses. In Figure 2, we show the spin–tilt misalignment for each of our six models of field binaries, overlaid with the (randomly distributed) misalignments for BBHs from clusters. As expected, both the fallback and proportional prescriptions show a decreasing spin–tilt misalignment as a function of binary chirp mass, defined as $\mathcal{M}_c \equiv (m_1 m_2)^{3/5}/(m_1 + m_2)^{1/5}$. Furthermore, for binaries that experience polar kicks, the spin–orbit misalignments are limited to $\theta_{LS} \lesssim 90^\circ$ for the full-NS kicks case, and $\theta_{LS} \lesssim 45^\circ$ for the fallback and proportional cases. This behavior is to be expected: in order to anti-align the orbital and spin angular momenta, the NKs must be able to reverse the orbital angular momentum, which is best accomplished by a planar kick with sufficient speed to reverse the orbital velocity. However, the

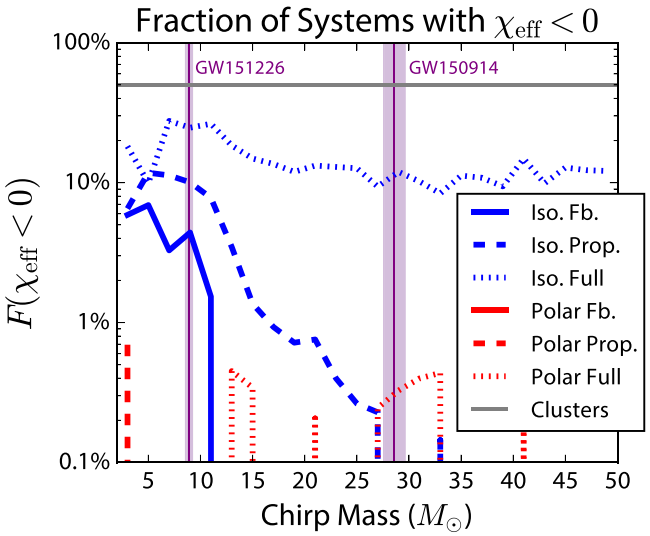

Figure 3. Fraction of binaries from each field model and from clusters with $\chi_{\rm eff} < 0$ as a function of chirp mass, with the median and 90% chirp masses of the two GW events in purple. Since cluster spin–tilts are distributed evenly in $\sin(\theta_{LS})$, half of all systems will have some component of the total spin anti-aligned with the orbital angular momentum. For field populations, the fraction of systems with $\chi_{\rm eff} < 0$ decreases as a function of mass. The only exception is the field model in which BHs are given fully isotropic kicks similar to neutron stars. In that case, 10%–30% of sources can have spins partially anti-aligned with $\hat{L}$, regardless of mass. For the polar kick models, only a handful of binaries show misalignments greater than 90°. This gives rise to the small spikes at ∼0.5% in the polar proportional and polar full kick models.

polar kick case explicitly excludes such planar kicks. The only exception would be the case where the first NK yields a misalignment $\theta_{LS} \sim 90°$, placing the second star in a position to emit an NK opposite to the direction of the orbital velocity. However, such large first kicks frequently unbind the binary, and any BBHs that survive are left with such large orbital separations that they will not merge within a Hubble time. The large tilts in the isotropic models are best understood by decomposing the kick into two components: a polar component that can torque the orbit up to 90, and a planar component, which can (in some cases) reverse the orbital velocity, flipping the orbit by 180. Because the planar kick component can be launched in a direction opposite the orbital velocity, the binary can be pushed into a tighter orbit, allowing it to merge within a Hubble time. On the other hand, the polar component of the kicks is always tangential to the orbit (for the first kick), increasing the orbital angular momentum and widening the orbit. This creates a bias for small NKs and correspondingly small tilts in the polar kick models, since only those systems will remain bound and merge within a Hubble time (as noted by Kalogera 2000).

Even when we allow for full-NS NKs independent of BH mass, the majority of systems do not show tilts beyond 90°. In Figure 3, we show the fraction of BBHs in each model that have spin–tilts greater than 90° as a function of chirp mass. For the polar kick models, less than 1% of binaries achieve a spin–orbit misalignment of greater than 90° at any given chirp mass. For isotropic kicks, the possibility of a spin–flip is significantly increased, since an isotropic distribution allows for the planar kicks required to reverse the orbital velocity. However, these kick magnitudes must be on the order of and in the opposite direction to the orbital velocity. For the isotropic fallback and isotropic proportional models, only 7% and 10% of the low-mass binaries ($\mathcal{M}_c \sim 5\,M_\odot$) have sufficient kicks to flip the orbital angular momentum. This fraction decreases as a function of mass, such that the isotropic fallback model produces *no* spin–orbit misalignments for $\mathcal{M}_c \gtrsim 11\,M_\odot$, while ∼1% of binaries with $\mathcal{M}_c \sim 15\,M_\odot$ can yield $\theta_{LS} > 90°$. Only the isotropic full-NS kick model can produce significant fractions (10%–30%) of anti-aligned heavy BBHs. For dynamically formed binaries, 50% of all systems show some anti-alignment of $\hat{S}$ and $\hat{L}$, as expected for systems whose angular momenta are isotropically distributed on the sphere.

4. DISCUSSION

Figure 3 illustrates a key point of this Letter: for sufficiently massive binaries, the most efficient way to produce systems with spin components anti-aligned with the orbital angular momentum is through dynamical encounters. Parameter estimation of the lower-mass BBH detected by Advanced LIGO, GW151226, suggests a chirp mass of $8.9^{+0.3}_{-0.3}\,M_\odot$ at the 90% credible level (Abbott et al. 2016d), and shows significant evidence for BH spins that are partially aligned with the orbital angular momentum. Given the analysis here, we cannot rule out either a field or dynamical formation scenario for GW151226. On the other hand, GW150914, the most massive BBH merger detected to date, was detected with a chirp mass of $28.1^{+1.8}_{-1.5}\,M_\odot$ at 90% confidence (Abbott et al. 2016c). Our results suggest that if a BBH similar to GW150914 were detected with a measurably negative $\chi_{\rm eff}$, it would strongly suggest a dynamical origin. Although parameter estimation of GW150914 hinted at such a configuration, with a measured an aligned-spin value of $\chi_{\rm eff} = -0.09^{+0.19}_{-0.17}$ at a 90% confidence, such a measurement does not definitively rule out either large, in-plane spins (which would also arise from dynamical formation) or small, aligned spins.

For systems similar to GW150914, Figure 2 shows that only full-NS NKs delivered in the plane of the orbit could produce a spin–orbit misalignment greater than 90°. However, we consider such kicks to be highly unlikely. Previous studies have indicated that such strong NKs would reduce the BBH merger rate from dense stellar environments by an order of magnitude (Rodriguez et al. 2016a), and from the field by two orders of magnitude (Dominik et al. 2013; Belczynski et al. 2016). Even under optimistic assumptions, this would yield a combined merger rate of BBHs in the local universe of $\sim 7\ {\rm Gpc^{-3}\ yr^{-1}}$, below the 90% lower limit of $9\ {\rm Gpc^{-3}yr^{-1}}$ reported from the first observing run of Advanced LIGO (Abbott et al. 2016d). We conclude that it is unlikely that BHs can receive such strong NKs across all mass ranges.

It should be mentioned that recent analyses of low-mass X-ray binaries (LMXBs) in the galaxy have suggested that while most BHs are consistent with no NKs at formation, at least a few BHs may receive NKs as high as $\sim 100\ {\rm km\ s^{-1}}$ (Podsiadlowski et al. 2002; Willems et al. 2005; Fragos et al. 2009; Repetto et al. 2012; Wong et al. 2012, 2014; Repetto & Nelemans 2015). In particular, Repetto & Nelemans (2015) noted that two LMXB systems, XTE J1118+48 and 0H1705-250, must have received kicks of at least $\sim 100\ {\rm km\ s^{-1}}$ and $\sim 450\ {\rm km\ s^{-1}}$, respectively, to explain their current positions in the galaxy; however, all of the NK prescriptions employed here can produce kicks of this magnitude for 5 $M_\odot$–10 $M_\odot$ BHs (see the Appendix; Figure 4), making our results consistent with the observed positions of these LMXBs. Furthermore, it has been shown that the estimated birth

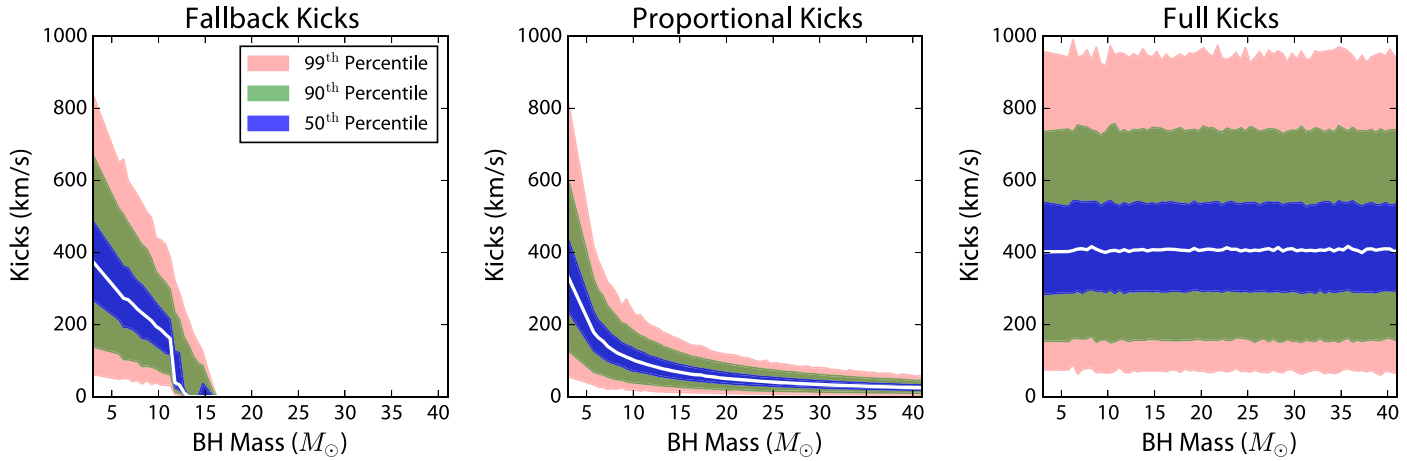

Figure 4. Distribution of kick magnitudes for each of our three models as a function of BH mass, for stars with initial masses from 20 $M_\odot$ to 150 $M_\odot$ at a metallicity of 0.1 $Z_\odot$. We include the median value and percentile regions for each 0.5 $M_\odot$ bin. The unusual behavior of the fallback prescription for BHs with masses between 11 $M_\odot$ and 15 $M_\odot$ arises from the SN prescription developed in Fryer et al. (2012; Section 4): BH progenitors with core masses from 6 $M_\odot$ to 7 $M_\odot$ experience full fallback of the SN ejecta, experiencing no NKs and producing BHs with masses in this range. But BH progenitors with core masses from 7 $M_\odot$ to 11 $M_\odot$ eject some fraction of their mass, enabling non-zero kicks and decreasing the mass of the resultant BH. This produces a bimodality in the fallback BH kicks.

velocity of H1705-250 can be explained by uncertainties in the observed position of the LMXB, without the need to invoke such large NKs (Mandel 2016).

Additionally, we have assumed that the amount of material that falls back on the proto-compact object will reduce the velocity of the BH via conservation of momentum. However, it has been suggested that the fallback of material can actually *accelerate* the BH to speeds similar to neutron stars, either via asymmetric accretion or though a gravitational "tug-boat" mechanism powered by the asymmetric ejecta (Janka 2013). However, such behavior would still only apply to BHs that eject some amount of material. For heavy BBHs such as GW150914, these prescriptions suggest that the BHs would form in a direct collapse with no significant mass ejecta (Fryer & Kalogera 2001; Belczynski et al. 2016). A direct collapse would also eliminate the possibility of an asymmetric SN altering the spin of the compact object itself (as has been invoked to explain the spin-misalignment of the double pulsar system PSR J07373039; Farr et al. 2011).

5. CONCLUSION

In this Letter, we explore the spin–tilt distributions of BBHs from different formation channels. We have shown for heavy BBH systems, such as GW150914, the allowed range of spin–orbit misalignments that can be produced by BH NKs is limited. Only under the extreme case where BHs of all masses can receive NKs comparable to NSs can isolated stellar evolution produce spin–tilt misalignment greater than 90°. On the other hand, BBHs formed through dynamical processes in dense star clusters are expected to produce isotropically distributed spin–tilt misalignments, which easily allow for the formation of BBHs with significantly anti-aligned spin and orbital angular momenta. Since any model of BH formation that allows for full-NS NKs results in a predicted BBH merger rate below the 90% lower limit observed by Advanced LIGO, we conclude that any sufficiently massive BBH merger ($\mathcal{M}_c \gtrsim 10$–$15\,M_\odot$, depending on the driving mechanism of the NK) that shows a negative $\chi_{\rm eff}$ was most likely formed through dynamical processes.

There are many additional facets of the BBH spin problem to be considered: first, although 50% of dynamically formed binaries will have $\chi_{\rm eff} < 0$ (assuming non-zero component spins), this does *not* mean that 50% of binaries detected by LIGO from clusters will have clearly discernible $\chi_{\rm eff} < 0$. Systems with $\chi_{\rm eff} \gg 0$ are detectable at greater distances than systems with $\chi_{\rm eff} \ll 0$ (Ajith et al. 2011; Dominik et al. 2015). Furthermore, systems with large spins in the plane of the orbit (the most probable configuration for dynamically formed binaries) will precess, producing amplitude modulations that can further decrease detectability of rapidly spinning binaries. Given that dynamics preferentially forms BBHs with spins lying in the orbital plane, such precessional effects may offer the best chance for identifying dynamically formed BBHs. Although precession has not been observed in the two BBHs detected so far, improvements in the lower-frequency limit of the LIGO instrument will increase the number of precessional periods a binary experiences while in the LIGO band, significantly improving the ability to measure the in-plane component of the BH spins. Studies to fully characterize the detection rate and distinguishability of these two astrophysical populations (similar to S. Stevenson & I. Mandel et al. 2016, in preparation; Vitale et al. 2016) are currently underway.

We thank Richard O'Shaughnessy, Chris Fryer, Will Farr, and Ilya Mandel for useful discussions, and Davide Gerosa for making the `Precession` package public. This work was supported by NSF grant AST-1312945, NSF grant PHY-1307020, and NASA grant NNX14AP92G. C.R. is grateful for the hospitality of the Kavli Institute for Theoretical Physics, NSF grant PHY11-25915, and is supported by the MIT Pappalardo Fellowship in Physics. V.K. and F.A.R. also acknowledge support from NSF grant PHY-1066293 at the Aspen Center for Physics.

APPENDIX
FIELD POPULATION

Since BSE does not track the full three-dimensional orientations of the spin or orbital angular momenta, we record the tilt of the orbit after the formation of each BH. This is done using the

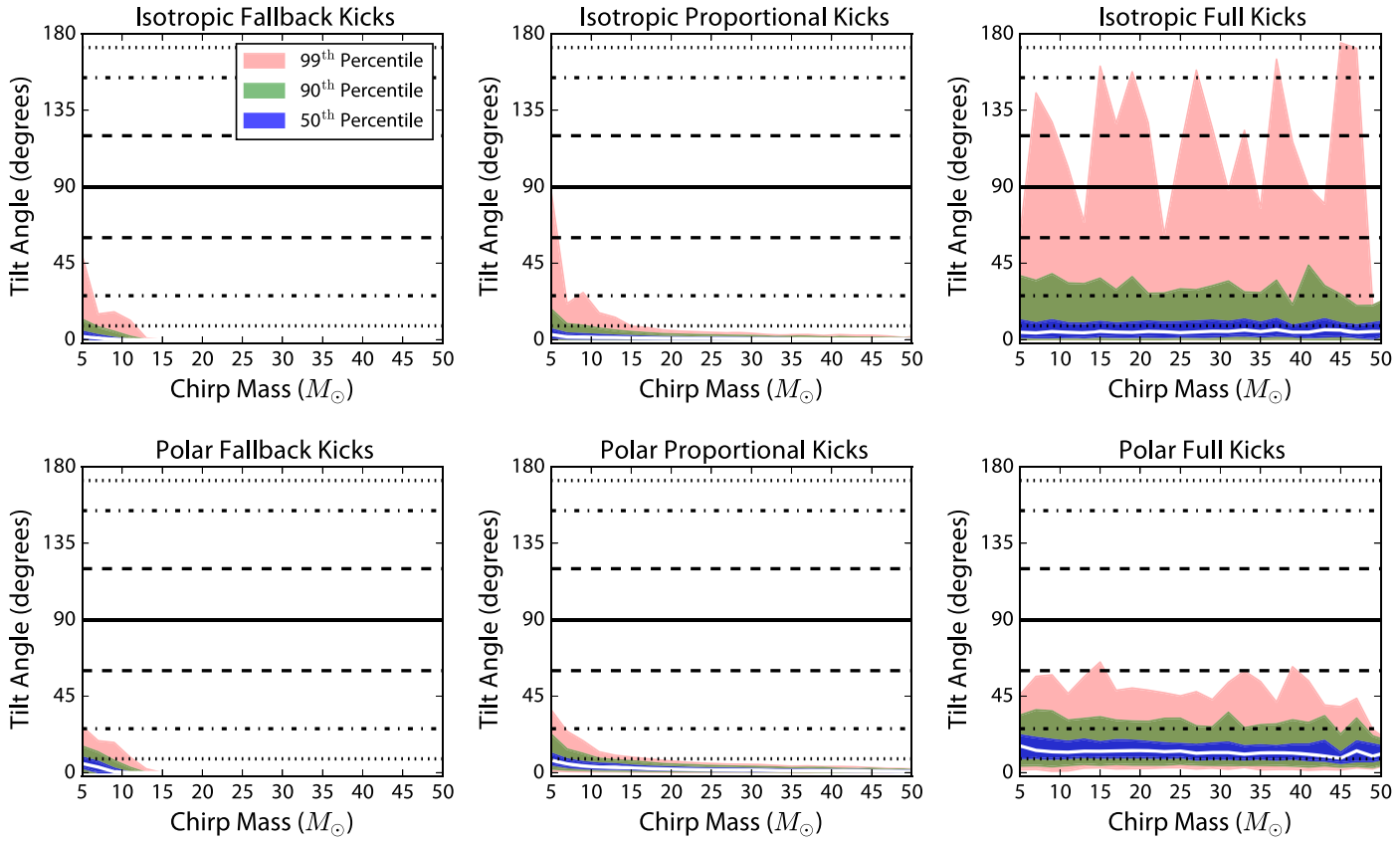

Figure 5. Similar to Figure 2, but now assuming that mass transfer and tidal torques can successfully realign $\boldsymbol{S}_1$ and $\boldsymbol{S}_2$ with $\hat{L}$ between the first and second SNe. Since the orbital velocities are significantly larger prior to the second collapse than prior to the first collapse, due to the decrease in separations following the common-envelope evolution, any NK for the second BH cannot change the orbit to the same degree as the first NK, preventing the large spin–tilts observed in Figure 2.

formalism developed in the appendix of the original BSE paper (Hurley et al. 2002). Briefly, when BSE applies a kick to a binary, it assumes a coordinate system with the non-exploding star at the origin and the exploding star placed a position r along the $\hat{y}$ axis. The instantaneous orbital velocity lies in the x–y plane and the orbital angular momentum vector, $\boldsymbol{L}$, points in the $\hat{z}$ direction. When the SN occurs, a kick is added to the orbital velocity, such that $\boldsymbol{V}_{\rm new} = \boldsymbol{V} + \boldsymbol{V}_{\rm kick}$. We show an example of the kick magnitudes for a single stellar metallicity in Figure 4. Since we assume that the NK is applied instantaneously on the orbital timescale of the binary, the separation does not change. The new direction of the orbital angular momentum vector is simply $\hat{L}_{\rm new} = \boldsymbol{r} \times \boldsymbol{V}_{\rm new}/|\boldsymbol{r} \times \boldsymbol{V}_{\rm new}|$, and the angle between the new and old angular momenta, ν, is $\cos(\nu) = \hat{L}_{\rm new} \cdot \hat{z}$.

Because BSE considers the orbit-averaged evolution of the binary, we can track the angle that $\hat{L}_{\rm new}$ makes with $\hat{L}$, but not the phase of the projection of $\hat{L}$ into the orbital plane. To that end, we select a random angle ϕ from 0 to 2π for the orbital phase of $\hat{L}$ in the new orbital plane. The total spin-misalignment is then

$$\cos\theta_{LS} = \cos(\nu_1)\cos(\nu_2) + \sin(\nu_1)\sin(\nu_2)\cos(\phi) \qquad (4)$$

where ν_1 and ν_2 are the tilts created after the first and second NKs. Note that this is identical to Equation (7) in Gerosa et al. (2013a). We assume that the timescale between the formation of the first and second BHs is sufficiently short that neither tides nor mass transfer can significantly realign the spin of the second star between the two SN. As such, our field binaries all have $\hat{S}_1 = \hat{S}_2$ by construction. This is considered a conservative assumption, as any physics which realigns $\boldsymbol{S}_1$ or $\boldsymbol{S}_2$ with $\boldsymbol{L}$ will necessary produce smaller tilts than those reported in the main text. As an illustration, we recreate Figure 2, assuming that both spins realign with the orbital angular momentum before the second BH forms (i.e., $\theta_{LS} = \nu_2$). See Figure 5.

REFERENCES

Abbott, B. P., Abbott, R., Abbott, T. D., et al. 2016a, PhRvL, 116, 241103
Abbott, B. P., Abbott, R., Abbott, T. D., et al. 2016b, PhRvL, 116, 061102
Abbott, B. P., Abbott, R., Abbott, T. D., et al. 2016c, PhRvL, 116, 241102
Abbott, B. P., Abbott, R., Abbott, T. D., et al. 2016d, PhRvX, 6, 041015
Ajith, P., Hannam, M., Husa, S., et al. 2011, PhRvL, 106, 241101
Antonini, F., & Perets, H. B. 2012, ApJ, 757, 27
Apostolatos, T., Cutler, C., Sussman, G., & Thorne, K. 1994, PhRvD, 49, 6274
Bartos, I., Kocsis, B., Haiman, Z., & Márka, S. 2016, arXiv:1602.03831
Belczynski, K., Dominik, M., Bulik, T., et al. 2010, ApJL, 715, L138
Belczynski, K., Holz, D. E., Bulik, T., & O'Shaughnessy, R. 2016, Natur, 534, 512
Bogdanovic, T., Reynolds, C., & Miller, C. 2007, ApJL, 661, L147
De Mink, S. E., & Mandel, I. 2016, MNRAS, 460, 3545
Dominik, M., Belczynski, K., Fryer, C., et al. 2012, ApJ, 759, 52
Dominik, M., Belczynski, K., Fryer, C., et al. 2013, ApJ, 779, 72
Dominik, M., Berti, E., O'Shaughnessy, R., et al. 2015, ApJ, 806, 263
Downing, J. M. B., Benacquista, M. J., Giersz, M., & Spurzem, R. 2010, MNRAS, 407, 1946
Downing, J. M. B., Benacquista, M. J., Giersz, M., & Spurzem, R. 2011, MNRAS, 416, 133
Farr, W. M., Kremer, K., Lyutikov, M., & Kalogera, V. 2011, ApJ, 742, 81
Fragos, T., Willems, B., Kalogera, V., et al. 2009, ApJ, 697, 1057
Fryer, C. L., Belczynski, K., Wiktorowicz, G., et al. 2012, ApJ, 749, 91
Fryer, C. L., & Kalogera, V. 2001, ApJ, 554, 548

Gerosa, D., & Kesden, M. 2016, PhRvD, 93, 124066
Gerosa, D., Kesden, M., Berti, E., O'Shaughnessy, R., & Sperhake, U. 2013a, PhRvD, 87, 104028
Gerosa, D., Kesden, M., Sperhake, U., Berti, E., & O'Shaughnessy, R. 2013b, PhRvD, 92, 064016
Gerosa, D., O'Shaughnessy, R., Kesden, M., Berti, E., & Sperhake, U. 2014, PhRvD, 89, 124025
Hobbs, G., Lorimer, D. R., Lyne, A. G., & Kramer, M. 2005, MNRAS, 360, 974
Hurley, J. R., Tout, C. A., & Pols, O. R. 2002, MNRAS, 329, 897
Janka, H.-T. 2013, MNRAS, 434, 1355
Kalogera, V. 2000, ApJ, 541, 319
Kaplan, D. L., Chatterjee, S., Gaensler, B. M., & Anderson, J. 2008, ApJ, 677, 1201
Kroupa, P. 2001, MNRAS, 322, 231
Mandel, I. 2016, MNRAS, 456, 578
Mandel, I., & De Mink, S. E. 2016, MNRAS, 458, 2634
Marchant, P., Langer, N., Podsiadlowski, P., Tauris, T. M., & Moriya, T. J. 2016, A&A, 588, A50
Ng, C. Y., & Romani, R. W. 2007, ApJ, 660, 37
Podsiadlowski, P., Nomoto, K., Maeda, K., et al. 2002, ApJ, 567, 491
Portegies Zwart, S. F., & Mcmillan, S. L. W. 2000, ApJL, 528, L17
Repetto, S., Davies, M. B., & Sigurdsson, S. 2012, MNRAS, 425, 2799
Repetto, S., & Nelemans, G. 2015, MNRAS, 453, 3341
Rodriguez, C. L., Chatterjee, S., & Rasio, F. A. 2016a, PhRvD, 93, 084029
Rodriguez, C. L., Haster, C.-J., Chatterjee, S., Kalogera, V., & Rasio, F. A. 2016b, ApJL, 824, L8
Rodriguez, C. L., Morscher, M., Pattabiraman, B., et al. 2015, PhRvL, 115, 051101
Sigurdsson, S., & Hernquist, L. 1993, Natur, 364, 423
Silsbee, K., & Tremaine, S. 2016, arXiv:1608.07642
Stone, N. C., Metzger, B. D., & Haiman, Z. 2016, arXiv:1602.04226v1
Trifirò, D., O'Shaughnessy, R., Gerosa, D., et al. 2016, PhRvD, 93, 044071
VanLandingham, J. H., Miller, M. C., Hamilton, D. P., & Richardson, D. C. 2016, ApJ, 828, 77
Vink, J. S., de Koter, A., & Lamers, H. J. G. L. M. 2001, A&A, 369, 574
Vitale, S., Lynch, R., Sturani, R., & Graff, P. 2016, arXiv:1503.04307v2
Vitale, S., Lynch, R., Veitch, J., Raymond, V., & Sturani, R. 2014, PhRvL, 112, 251101
Voss, R., & Tauris, T. M. 2003, MNRAS, 342, 1169
Wang, C., Lai, D., & Han, J. L. 2006, ApJ, 639, 1007
Willems, B., Henninger, M., Levin, T., et al. 2005, ApJ, 625, 324
Wong, T.-W., Valsecchi, F., Ansari, A., et al. 2014, ApJ, 790, 119
Wong, T.-W., Valsecchi, F., Fragos, T., & Kalogera, V. 2012, ApJ, 747, 111
Ziosi, B. M., Mapelli, M., Branchesi, M., & Tormen, G. 2014, MNRAS, 441, 3703